Supplementary Material

Novel multi-omics deconfounding variational autoencoders can obtain meaningful disease subtyping

Zuqi Li[1,†], Sonja Katz[2,3,4,†], Edoardo Saccenti[3], David W. Fardo[5], Peter Claes[6,7,8], Vitor A.P. Martins dos Santos[4,9], Kristel Van Steen[1,10], Gennady V. Roshchupkin[2,11,*]

[1]BIO3 - Laboratory for Systems Medicine, Department of Human Genetics, KU Leuven, Leuven, Belgium.

[2]Department of Radiology and Nuclear Medicine, Erasmus MC, Rotterdam, The Netherlands.

[3]Laboratory of Systems and Synthetic Biology, Wageningen University & Research, Wageningen, The Netherlands.

[4]LifeGlimmer GmbH, Berlin, Germany.

[5]University of Kentucky, Lexington, The United States.

[6]Department of Human Genetics, KU Leuven, Leuven, Belgium.

[7]Medical Imaging Research Center, University Hospitals Leuven, Leuven, Belgium.

[8]Department of Electrical Engineering, ESAT-PSI, KU Leuven, Leuven, Belgium

[9]Laboratory of Bioprocess Engineering, Wageningen University & Research, Wageningen, The Netherlands.

[10]BIO3 - Laboratory for Systems Genetics, GIGA Molecular & Computational Biology, University of Liège, Liège, Belgium.

[11]Department of Epidemiology, Erasmus MC, Rotterdam, The Netherlands.

g.roshchupkin@erasmusmc.nl

†Authors contributed equally *Corresponding author

1 Supplementary Results

1.1 Visualization: Performances of deconfounding strategies

1.1.1 Single confounder simulations

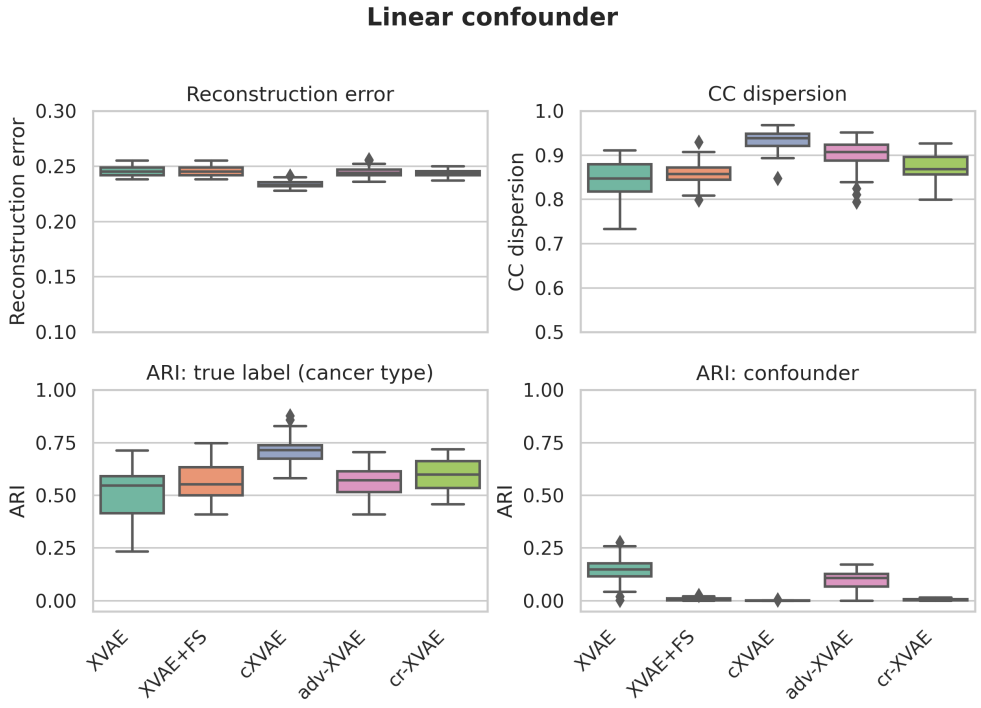

Supplementary Figure 1: **Overview performances of deconfounding strategy for single confounder simulations**. Boxplots of 50 runs with different parameter initialisation and randomly sampled training and validation data. Models abbreviations designate the following deconfounding strategies and implementations thereof: vanilla XVAE without any deconfounding (XVAE), XVAE with feature selection in the form of removing correlated latent features (XVAE+FS, correlation cutoff = 0.5), conditional XVAE (cXVAE, input + embedding), adversarial training with XVAE (adv-XVAE, multiclass MLP), confounder-regularised XVAE (cr-XAVE, squared correlation regularisation). Reconstruction error: relative error in the reconstruction of X1 and X2 weighted eqally; CC dispersion: consensus clustering agreement over 50 iterations; True clustering: adjusted rand index (ARI) of consensus clustering derived clusters with True label labels; Confounder clustering: ARI of consensus clustering derived clusters with simulated confounder labels. More details can be found in Table 1 of the main manuscript.

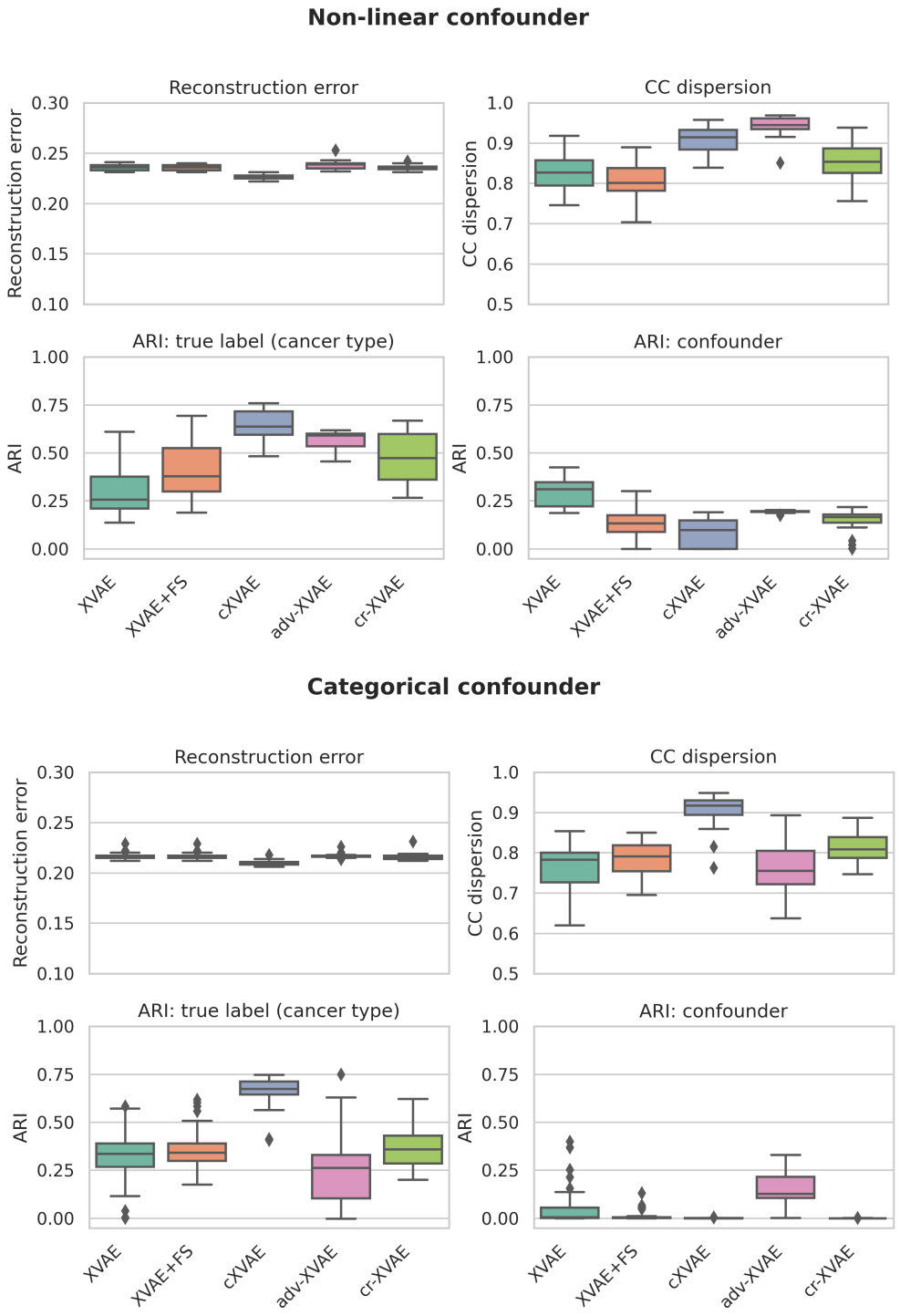

Supplementary Figure 1: **Overview performances of deconfounding strategy for single confounder simulations** (cont.)

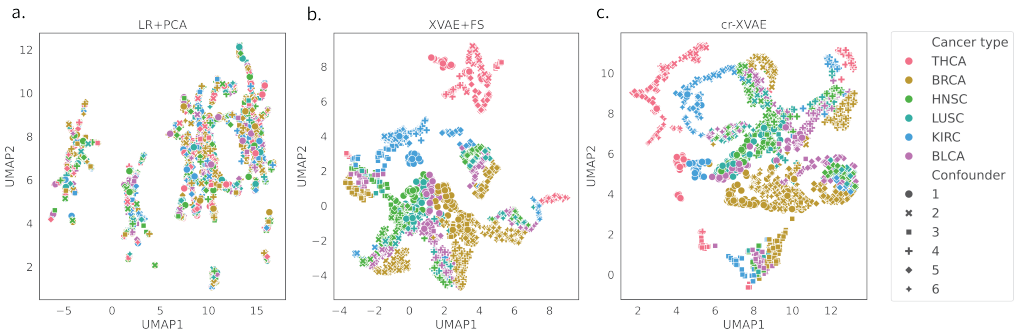

Supplementary Figure 2: **Deconfounding behaviour of several developed models**. Dimensionality reduction (UMAP) plot of the deconfounding using the models (a.) LR+PCA, (b.) XVAE+FS, or (c.) cr-XVAE. Marker colors indicate the true label labels (i.e. TCGA cancer types), while marker shapes indicate the six classes (1-6) of the confounder (see section 2.2). This figure is an extension to the information displayed in Figure 4.

1.1.2 Multiple confounder simulations

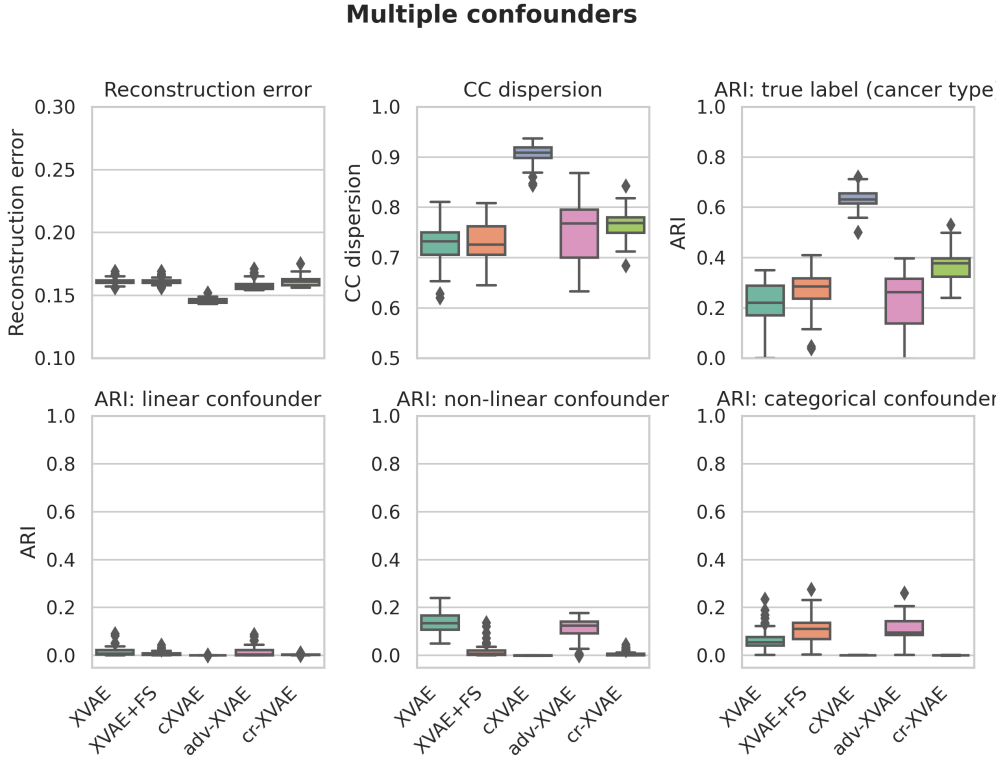

Supplementary Figure 3: **Overview performances of deconfounding strategy in the presence of multiple confounders**. Values are displayed as mean ± standard deviation of 50 runs with different parameter initialisation and randomly sampled training and validation data. More details can be found in Table 2 of the main manuscript.

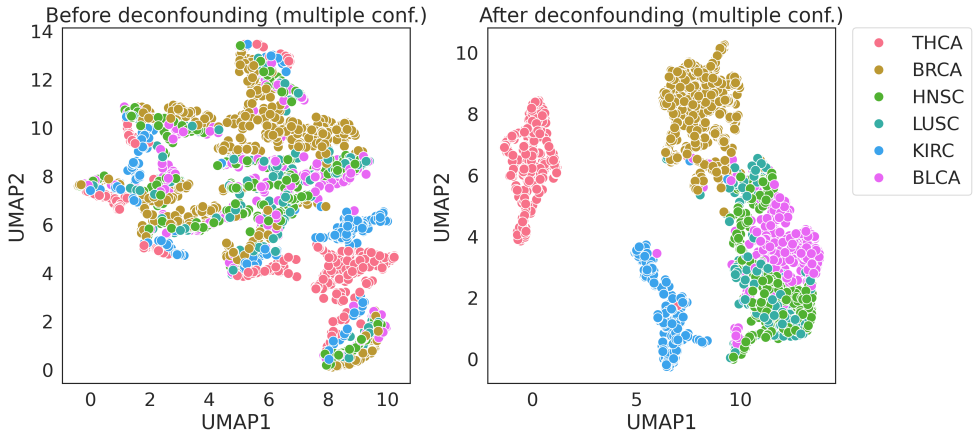

Supplementary Figure 4: **Deconfounding behaviour of cXVAE in the presence of multiple confounders**. Dimensionality reduction (UMAP) plot of multiple confounded data before (left) and after (right) application of cXVAE. Marker colors indicate the true label labels (i.e. TCGA cancer types).

1.2 Cancer subtype analysis

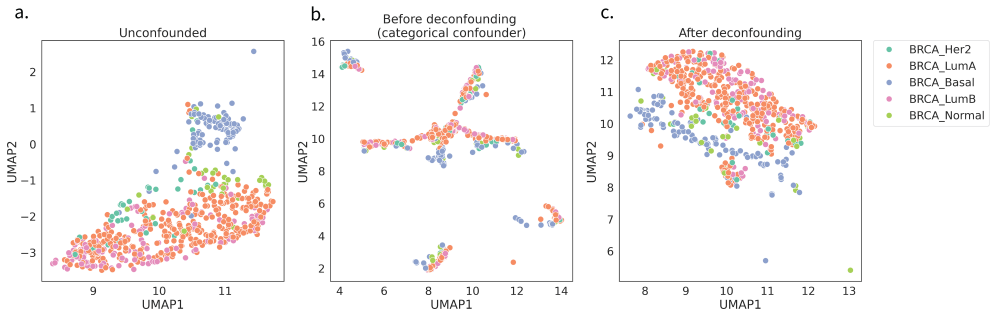

Supplementary Figure 5: **Breast cancer subtypes are conserved after deconfounding with cXVAE**. (a.) UMAP of TCGA-BRCA samples (b.) TCGA-BRCA samples after categorical confounding (see Material and Methods section 2.2.3 for more details). (c.) Categorically confounded TCGA-BRCA samples after deconfounding using cXVAE. Colours indicate the BRCA subtypes Her2, LumA, Basal, LumB, and normal.

1.3 Differences in model implementations have significant impact on deconfounding performance

Each of the deconfounding strategies compared in this study has a number of possible implementations for both single and multiple confounder simulations (Supplementary Table 2), which we observed to have a major impact on model performances. Hence,

in this section, we sequentially discuss each strategy, highlighting the most notable differences between implementations and providing readers with recommendations on designing similar frameworks.

XVAE with feature selection (XVAE+FS) - the central question when conducting feature selection by removing latent features correlated with unwanted confounders is the correlation cutoff employed. We compared the use of two different correlation cutoffs (Pearson correlation > 0.5, correlation > 0.3) and using a significant p-value as cutoff (p-value <0.05). While using absolute correlations as threshold removed up to 30% of latent features, using the p-value commonly removed >90% of features, rendering the latent space too sparse to use.

Conditional XVAE (cXVAE) - cXVAE may vary regarding which layer of the autoencoder confounders are added, and whether they are added in both the encoder and decoder of the autoencoder. We found that in general it does not affect the deconfounding performance of the network in which layer of the encoder confounders are added (Supplementary Table 2, *input + embedding*, *fused + embedding*). We hypothesised that it may suffice to only add confounders to the encoder, however we found that a decoder lacking confounders (*input*) performs significantly worse. Conversely, adding the conditional variable to only the decoder results in good deconfounding performances (*embed*).

Adversarial training (adv-XVAE) - while the possibilities to design adversarial training strategies are countless, we found it challenging to tune hyperparameters and balance the regularisation terms to simultaneously achieve good reconstruction and satisfactory deconfounding. Bahrami et al. [1] proposed a variation in which a simplified loss function is backpropagated solely through the encoder of the network, to reinforce deconfounding (*scGAN*). However, we found this modified version could not deliver more consistent results. We attempted to extend the original model to accommodate multiple confounders by incorporating one adversarial network for each confounder present (*multinet MLP*). Contrary to expectations however, this implementations failed to improve adversarial training performance for the multiple confounder simulations (Supplementary Table 3).

Confounder regularised XVAE (cr-XVAE) - the regularisation term added for our deconfounding regularisation strategy largely determines the deconfounding properties.

As a general guideline, Pearson correlation accounts for linear associations whereas mutual information can capture higher-level dependencies. Because we are only interested in the strength of correlation, not the sign, the correlation coefficient was converted into absolute value or squared, leading to slightly different performances (Supplementary Table 2). Meanwhile, we conducted two different implementations for mutual information as loss function to approximate latent feature distribution, one based on differentiable histogram and the other on kernel density estimate. For both methods, the regularisation quality relies on how good the approximation is.

1.4 Deconfounding approaches should be motivated by the nature of confounders

Our results revealed that methods differentiate themselves regarding the trade-off they achieve between removing confounding signal and maintaining true patient clustering. Accordingly, we categorised all surveyed deconfounding approaches in either *aggressive* or *preserving* methods.

Aggressive methods, e.g., removing latent features correlated with confounders, or enforcing deconfounding in the objective function, tend to efficiently remove confounders, however, at the cost of biological signal. While this stringent approach resulted in intermediate true clustering accuracy in our study, the remaining true signal will likely contain strong true positive findings.

Preserving methods, including cXVAE and adversarial training, tend not to remove confounders at all costs, which generally yielded higher true clustering accuracy, but also a higher fraction of deconfounding signal remained in the data.

We argue that aggressive methods are best applied in the case of technical confounders, like batch effects, in which not removing all of the confounding signal may easily lead to spurious biological conclusions [2, 3]. Preserving methods, on the other hand, are interesting for removing biological confounders, e.g. sex or age effects, as applying a too stringent method may lead to removing too much (weak) biological signal of interest. However, this comes at the risk of findings containing more false positives, so thorough validation of results is advised.

Notably, we observed that simply training an autoencoder on confounded data may

already lead to deconfounding, which is grounded in the inability of the autoencoder to fully model the confounder. Nevertheless, the obscuring effect of confounders on the true clustering can not be removed by a vanilla autoencoder, underlying the need for extraneous deconfounding approaches.

2 Supplementary Methods

2.1 Visualization of confounder simulations

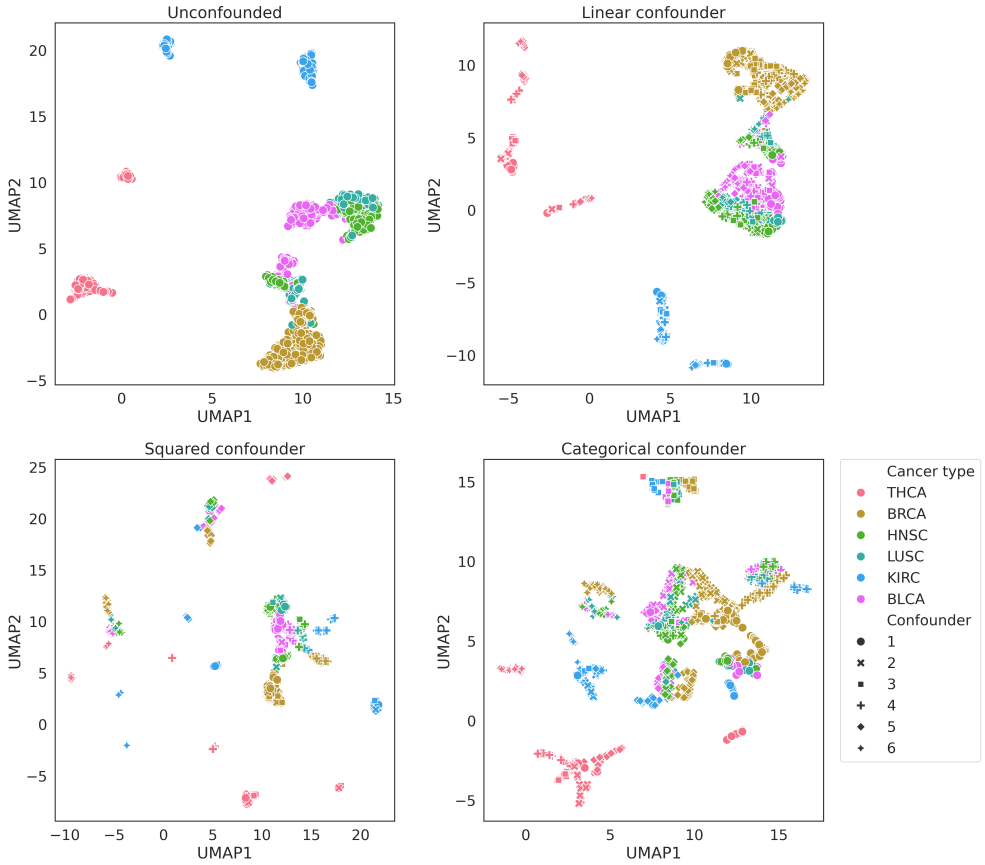

Supplementary Figure 6: Dimensionality reduction (UMAP) plots of unconfounded (upper left), linear confounded (upper right), non-linear confounded (lower left), and categorical confounded (lower right) data. Colors indicate the true labels (i.e. TCGA cancer types), while shapes indicate the six different simulated confounders

2.2 Variational autoencoder for data integration (XVAE)

Autoencoders (AE) are unsupervised neural networks consisting of an encoder and a decoder part. While the encoder (E_ϕ, parameterised by ϕ) maps the high dimensional input datapoint (x) into a lower dimensional latent embedding (z), the decoder (D_θ, parameterised by θ) attempts to reconstruct the original input from the embedding ($x' = D_\theta(z) = D_\theta(E_\phi(x))$).

The network is then trained by trying to minimize the error between original input and

reconstruction, quantified by the mean squared error:

$$L_{\mathrm{AE}}(\phi, \theta; x) = \|x - x'\|^2 = \|x - D_\theta(z)\|^2 = \|x - D_\theta(E_\phi(x))\|^2 \tag{1}$$

Standard autoencoders have demonstrated shortcomings in terms of generative abilities and the tendency to over-fit input data due to their lack of regularization. These limitations are addressed by a popular variant of autoencoder, termed variational autoencoder (VAE), which encodes input variables as a probability distribution ($q_\phi(z|x)$) over the latent space rather than as a fixed value [4]. For the sake of easy computation and interpretation, the typical choice is to assume the latent distribution $q_\phi(z|x)$ as a Gaussian distribution. The unsupervised encoder-decoder structure allows (variational) autoencoders to act as dimensionality reduction and clustering tools, capable of accommodating input data from different sources in a joint low-dimensional embedding, ultimately making them a popular tool for data integration. Following the originally proposed implementation, we used a combined loss function of the Mean Squared Error (MSE) for scoring the reconstruction loss and Maximum Mean Discrepancy (MMD) as regularization term, balanced by the constant beta (β), which was set to 1 for all experiments:

$$L_{\mathrm{VAE}}(\phi, \theta; x) = -E_{z \sim q_\phi(z|x)}[\log p_\theta(x|z)] + \beta * \mathrm{MMD}(q_\phi(z|x)||p(z)) \tag{2}$$

For the activation function, we chose the Leaky Rectified Linear Unit activation function (LeakyReLU) [5] in all layers except the output layer, which employs a sigmoid activation function. We are able to use the sigmoid function due to the normalisation of every mRNA and DNAm feature to the range $[0, 1]$ during preprocessing. To enhance training stability, batch normalisation layers are added to the encoder. We trained every model for a fixed period of 150 epochs using an Adam optimiser [6] and a batch size of 64. To derive an optimal architecture for the XVAE base model, we carried out a hyperparameter search assessing the combination of (1) the number of nodes in hidden layers and latent embedding, (2) the rate of dropout layers, and (3) the weight initialisation.

2.3 cXVAE: Conditional XVAE

While traditionally auxiliary variables are added in the encoder and decoder, in theory this can be varied. To investigate the impact of deconfounding attributable to when confounders are added to the model, we created several variations of the cXVAE architecture (Supplementary Figure 7):

1. *input* - in the encoder confounders are concatenated with the input vector; no addition of confounders in the decoder.

2. *embed* - in the decoder confounders are concatenated with the latent embedding; no addition of confounders in the encoder.

3. *input + embedding* - in the encoder confounders are concatenated with the input vector; in the decoder confounders are concatenated with the latent embedding.

4. *fused + embedding* - in the encoder confounders are concatenated in the second hidden layer, where the fusion of data types occurs; in the decoder confounders are concatenated with the latent embedding.

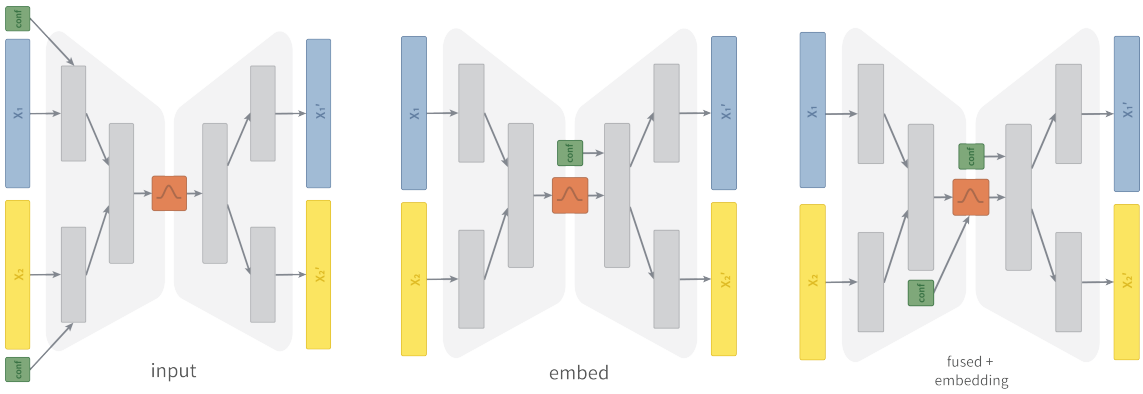

Supplementary Figure 7: Overview on the different cXVAE assessed in this study.

2.4 adv-XVAE: XVAE with adversarial training

As an adversarial network we implement a simple multi-layer perceptron (MLP) with two layers. The first layer takes the generated embedding of the XVAE model as input and applies ReLU activation to condense it to 10 features. The output of the second

layer features the number of confounders to be predicted and uses the activation function fitting for predicting respective confounder; i.e. uses ReLU in case of continuous confounders, a sigmoid activation function in case of binary confounders, and softmax activation for multiple categorical confounders.

The training procedure can be broken down in three steps:

(i) Pre-train the XVAE: we pre-train the XVAE model for 5 epochs optimising equation 9.

(ii) Pre-train the adversarial network: we use the latent embedding initialized in (i) to pre-train the adversarial network for 5 epochs using a loss function fitting the numerical type of confounder (mean squared error for continuous, binary cross entropy for binary, and cross entropy for categorical confounders), i.e. $L_{\text{adv}}(h_\nu(x), c)$ where h_ν denotes the adversarial network parameterized by ν.

(iii) Joint adversarial training: joint training is unique in its attempt to minimize the XVAE loss (Formula 9) while simultaneously maximizing the adversarial network loss through a combined loss function:

$$L_{\text{adv}-\text{XVAE}}(\phi, \theta, \nu; x, c) = L_{\text{XVAE}}(\phi, \theta; x) - \lambda L_{\text{adv}}(h_v(x), c) \tag{3}$$

Training is carried out in a ping-pong fashion, where firstly all weights of the adversarial network are frozen and the autoencoder trained for one epoch optimizing Formula 2, followed by the freezing of autoencoder weights and training of the adversary network for an entire epoch to minimize the adversarial network prediction loss L_{adv}.

Depending on how the adversarial architecture is designed in the case of multiple confounders present, we differentiate two major variations of the above described base model: *multiclass MLP* and *multinet MLP*.

In *multiclass MLP* adversarial networks confounders are concatenated to a combined label, effectively creating a (mixed) multiclass classification problem. To successfully predict labels of different numeric nature, instead of a single final layer, multiclass MLP feature up to three final layers, each with different activation functions (ReLU for nu-

merical confounders, sigmoid for binary categorical confounders, softmax for categorical confounders with more than one class).

Multinet MLP, on the other hand, possesses an individual adversarial MLP for each confounder variable. The adversarial loss L_{adv} becomes the sum of losses of these individual networks.

Instead of augmenting the architecture of their *scGAN* model, Bahrami et al. [1] proposed changes to the training procedure. While following the same initial strategy of separately pre-training the autoencoder and adversarial MLP, they simplified the overall objective function (Formula 3) by omitting the autoencoder loss and instead only training the encoder by maximizing the adversarial prediction loss L_{adv}.

References

[1] Mojtaba Bahrami, Malosree Maitra, Corina Nagy, Gustavo Turecki, Hamid R Rabiee, and Yue Li. Deep feature extraction of single-cell transcriptomes by generative adversarial network. *Bioinformatics*, 37(10):1345–1351, June 2021.

[2] Wilson Wen Bin Goh, Wei Wang, and Limsoon Wong. Why Batch Effects Matter in Omics Data, and How to Avoid Them. *Trends in Biotechnology*, 35(6):498–507, June 2017.

[3] Jelena Čuklina, Patrick G. A. Pedrioli, and Ruedi Aebersold. Review of Batch Effects Prevention, Diagnostics, and Correction Approaches. In Rune Matthiesen, editor, *Mass Spectrometry Data Analysis in Proteomics*, Methods in Molecular Biology, pages 373–387. Springer, New York, NY, 2020.

[4] Diederik P Kingma and Max Welling. Auto-encoding variational bayes. *arXiv preprint arXiv:1312.6114*, 2013.

[5] Bing Xu, Naiyan Wang, Tianqi Chen, and Mu Li. Empirical evaluation of rectified activations in convolutional network. *arXiv preprint arXiv:1505.00853*, 2015.

[6] Diederik P Kingma and Jimmy Ba. Adam: A method for stochastic optimization. *arXiv preprint arXiv:1412.6980*, 2014.

3 Supplementary Tables

206

linear confounder

		reconstruction error			CC	Internal clustering		True clustering		Confounder clustering	
		X1	X2	X1,X2	dispersion	Silhouette	DB index	ARI	NMI	ARI	NMI
XVAE	mean	0.303	0.222	0.246	0.844	0.120	2.114	0.506	0.594	1.51E-01	2.02E-01
	std	0.010	0.003	0.004	0.045	0.013	0.118	0.116	0.093	5.71E-02	7.13E-02
XVAE + FS	mean	0.302	0.222	0.245	0.860	0.131	2.076	0.571	0.686	7.70E-03	1.14E-02
	std	0.010	0.003	0.004	0.028	0.011	0.146	0.092	0.053	6.79E-03	7.44E-03
cXVAE	mean	0.286	0.212	0.234	0.935	0.133	2.243	0.712	0.786	4.82E-04	3.11E-03
	std	0.008	0.001	0.003	0.023	0.011	0.092	0.055	0.037	5.37E-04	7.02E-04
adv-XVAE	mean	0.302	0.221	0.245	0.901	0.143	2.013	0.568	0.666	9.34E-02	1.28E-01
	std	0.010	0.003	0.004	0.032	0.011	0.099	0.070	0.053	5.14E-02	6.60E-02
cr-XVAE	mean	0.300	0.221	0.244	0.873	0.129	2.133	0.598	0.715	4.18E-03	6.97E-03
	std	0.007	0.002	0.003	0.028	0.010	0.123	0.074	0.046	3.91E-03	3.97E-03

non-linear confounder

		reconstruction error			CC	Internal clustering		True clustering		Confounder clustering	
		X1	X2	X1,X2	dispersion	Silhouette	DB index	ARI	NMI	ARI	NMI
XVAE	mean	0.235	0.236	0.236	0.826	0.119	2.078	0.307	0.424	2.97E-01	3.71E-01
	std	0.005	0.002	0.003	0.042	0.011	0.099	0.141	0.120	7.07E-02	8.17E-02
XVAE + FS	mean	0.235	0.236	0.236	0.805	0.114	2.120	0.411	0.526	1.38E-01	1.84E-01
	std	0.005	0.002	0.003	0.040	0.011	0.111	0.142	0.123	7.80E-02	9.75E-02
cXVAE	mean	0.223	0.229	0.227	0.908	0.124	2.185	0.646	0.713	7.59E-02	1.06E-01
	std	0.005	0.001	0.002	0.031	0.012	0.070	0.079	0.076	7.36E-02	9.87E-02
adv-XVAE	mean	0.240	0.237	0.238	0.942	0.147	1.918	0.568	0.635	0.194	0.249
	std	0.010	0.002	0.004	0.025	0.012	0.090	0.049	0.032	0.006	0.007
cr-XVAE	mean	0.235	0.235	0.235	0.852	0.121	2.092	0.478	0.575	1.54E-01	2.08E-01
	std	0.005	0.001	0.002	0.043	0.011	0.094	0.129	0.092	4.15E-02	5.24E-02

Supplementary Table 1: **Overview performances of deconfounding strategy for single confounder simulations**. Values are displayed as mean (mean) and standard deviation (std) of 50 runs with different initialisation. Models on the first column indicate the following deconfounding strategies and implementations thereof: vanilla XVAE without any deconfounding (XVAE), XVAE with feature selection in the form of removing correlated latent features (XVAE+FS, correlation cutoff = 0.5), conditional XVAE (cXVAE, input + embedding), adversarial training with XVAE (adv-XVAE, multiclass MLP), confounder-regularised XVAE (cr-XAVE, squared correlation regularisation). Reconstruction error: relative error in the reconstruction of X1 and/or X2; CC dispersion: consensus clustering agreement over 50 iterations; Internal clustering: Silhouette score and Davies-Bouldin (DB) index of consensus clustering derived clusters without label information; True clustering: adjusted rand index (ARI) and Normalized Mutual Information (NMI) of consensus clustering derived clusters with ground-truth labels; Confounder clustering: ARI and NMI of consensus clustering derived clusters with simulated confounder labels.

categorical confounder

		reconstruction error			CC	Internal clustering		True clustering		Confounder clustering	
		X1	X2	X1,X2	dispersion	Silhouette	DB index	ARI	NMI	ARI	NMI
XVAE	mean	0.205	0.224	0.216	0.762	0.085	2.379	0.330	0.431	4.85E-02	9.12E-02
	std	0.006	0.002	0.003	0.055	0.008	0.073	0.125	0.148	8.80E-02	1.44E-01
XVAE + FS	mean	0.205	0.224	0.216	0.787	0.084	2.327	0.361	0.473	9.53E-03	2.02E-02
	std	0.006	0.002	0.003	0.040	0.008	0.087	0.100	0.099	2.31E-02	4.50E-02
cXVAE	mean	0.197	0.218	0.210	0.911	0.117	2.311	0.664	0.738	4.67E-04	3.17E-03
	std	0.003	0.001	0.002	0.033	0.011	0.084	0.070	0.060	9.62E-04	1.34E-03
adv-XVAE	mean	0.205	0.224	0.217	0.764	0.121	2.168	0.240	0.273	1.56E-01	3.12E-01
	std	0.003	0.001	0.002	0.058	0.008	0.050	0.188	0.203	8.40E-02	1.60E-01
cr-XVAE	mean	0.204	0.224	0.216	0.813	0.109	2.077	0.368	0.490	-9.12E-05	2.55E-03
	std	0.005	0.002	0.003	0.034	0.011	0.091	0.101	0.098	6.09E-04	7.96E-04

Supplementary Table 2: **Overview performances of deconfounding strategy for single confounder simulations** - continued

Supplementary Table 2: **Performance overview of different implementations of each deconfounding strategy for single confounders**

linear confounder

	Implementation	Reconstruction error			CC	Clustering performance: Internal		True label		Confounder	
		X1	X2	X1,X2	dispersion	Silhouette	DB index	ARI	NMI	ARI	NMI
baseline	XVAE (unconfounded)	0.438	0.278	0.31	0.957	0.128	2.17	0.731	0.821	1.14E-04	2.60E-03
	KMeans	-	-	-	-	0.132	2.14	0.212	0.381	3.53E-01	5.15E-01
	PCA(50) + KMeans	-	-	-	-	0.189	1.66	0.211	0.381	3.54E-01	5.17E-01
	LR + PCA + KMeans	-	-	-	-	0.251	1.80	0.692	0.763	1.50E-04	2.66E-03
	XVAE	0.294	0.22	0.241	0.807	0.11	2.25	0.411	0.522	2.08E-01	2.93E-01
XVAE + FS	XVAE (corr 0.3)	0.294	0.220	0.241	0.843	0.133	2.12	0.561	0.634	6.54E-03	1.13E-02
	XVAE (corr 0.5)	0.294	0.220	0.241	0.868	0.124	2.22	0.617	0.710	4.73E-03	8.51E-03
	XVAE (pVal 0.05)	0.294	0.220	0.241	0.653	0.160	1.66	0.261	0.354	3.38E-02	4.96E-02
cXVAE	input	0.29	0.217	0.238	0.907	0.111	2.06	0.429	0.582	1.84E-01	2.23E-01
	inputEmbed	0.281	0.212	0.233	0.895	0.147	2.21	0.715	0.768	4.72E-04	3.13E-03
	embed	0.285	0.215	0.235	0.931	0.146	2.20	0.702	0.769	4.87E-04	3.06E-03
	fusedEmbed	0.282	0.212	0.233	0.933	0.127	2.26	0.718	0.764	5.41E-04	3.15E-03
adv-XVAE	multiclass	0.289	0.217	0.238	0.920	0.142	2.16	0.632	0.723	3.46E-03	6.98E-03
	multiclass (1batch)	0.358	0.272	0.297	0.867	0.150	1.79	0.368	0.509	1.62E-01	3.05E-01
	multiclass (scGAN)	0.287	0.214	0.235	0.940	0.125	2.26	0.739	0.821	2.23E-04	2.93E-03
	multinet	0.289	0.217	0.238	0.920	0.142	2.16	0.632	0.723	3.46E-03	6.98E-03
cr-XVAE	corrSq	0.302	0.223	0.246	0.871	0.133	2.02	0.549	0.673	7.17E-03	9.80E-03
	corrAbs	0.292	0.218	0.239	0.921	0.134	2.23	0.692	0.779	1.93E-04	2.95E-03
	MIhist	0.295	0.219	0.241	0.838	0.089	2.21	0.273	0.377	2.88E-01	3.59E-01
	MIKDE	0.294	0.22	0.241	0.814	0.115	2.24	0.513	0.671	3.66E-03	6.00E-03

non-linear confounder

	Implementation	Reconstruction error			CC	Clustering performance: Internal		True label		Confounder	
		X1	X2	X1,X2	dispersion	Silhouette	DB index	ARI	NMI	ARI	NMI
baseline	XVAE (unconfounded)	0.438	0.278	0.31	0.957	0.128	2.17	0.731	0.821	1.14E-04	2.60E-03
	KMeans	-	-	-	-	0.160	1.82	0.251	0.411	3.25E-01	4.90E-01
	PCA(50) + KMeans	-	-	-	-	0.222	1.44	0.252	0.412	3.24E-01	4.89E-01
	LR + PCA + KMeans	-	-	-	-	0.242	1.48	0.391	0.567	2.15E-01	3.65E-01
	XVAE	0.227	0.234	0.232	0.846	0.123	2	0.153	0.293	4.00E-01	4.88E-01
XVAE + FS	XVAE (corr 0.3)	0.227	0.234	0.232	0.725	0.113	2.02	0.322	0.485	9.10E-02	1.16E-01
	XVAE (corr 0.5)	0.227	0.234	0.232	0.784	0.113	2.09	0.464	0.592	4.40E-02	5.30E-02
	XVAE (pVal 0.05)	0.227	0.234	0.232	0.721	0.192	1.44	0.226	0.308	1.16E-01	1.90E-01
cXVAE	input	0.224	0.233	0.23	0.956	0.146	1.96	0.477	0.598	1.95E-01	2.56E-01
	inputEmbed	0.217	0.23	0.225	0.867	0.145	2.18	0.758	0.788	8.64E-05	2.64E-03
	embed	0.216	0.229	0.224	0.832	0.114	2.22	0.498	0.576	1.34E-01	1.82E-01
	fusedEmbed	0.219	0.229	0.224	0.909	0.128	2.08	0.612	0.671	1.69E-01	2.20E-01
adv-XVAE	multiclass	0.229	0.235	0.233	0.951	0.144	1.930	0.559	0.637	1.97E-01	2.52E-01
	multiclass (1batch)	0.282	0.293	0.289	0.877	0.164	1.700	0.401	0.532	1.61E-01	3.27E-01
	multiclass (scGAN)	0.223	0.230	0.228	0.900	0.107	2.290	0.543	0.638	1.81E-01	2.37E-01
	multinet	0.229	0.245	0.233	0.951	0.144	1.930	0.559	0.637	1.97E-01	2.52E-01
cr-XVAE	corrSq	0.227	0.234	0.232	0.857	0.126	2.08	0.361	0.51	1.34E-01	1.93E-01
	corrAbs	0.226	0.234	0.232	0.818	0.118	2.03	0.334	0.496	1.67E-01	2.24E-01
	MIhist	0.228	0.236	0.233	0.867	0.126	2.01	0.336	0.493	1.91E-01	2.59E-01
	MIKDE	0.227	0.234	0.231	0.852	0.117	2.10	0.337	0.487	1.92E-01	2.53E-01

Supplementary Table 2: **Performance overview of different implementations of each deconfounding strategy for single confounders** - continued

categorical confounder

	Implementation	Reconstruction error			CC	Clustering performance: Internal		True label		Confounder	
		X1	X2	X1,X2	dispersion	Silhouette	DB index	ARI	NMI	ARI	NMI
baseline	XVAE (unconfounded)	0.438	0.278	0.31	0.957	0.128	2.17	0.731	0.821	1.14E-04	2.60E-03
	KMeans	-	-	-	-	0.150	1.91	0.0610	0.117	2.18E-01	3.71E-01
	PCA(50) + KMeans	-	-	-	-	0.197	1.62	0.0631	0.120	2.15E-01	3.68E-01
	LR + PCA + KMeans	-	-	-	-	0.186	1.71	0.150	0.269	7.09E-02	1.52E-01
	XVAE	0.203	0.225	0.217	0.755	0.0819	2.32	0.335	0.476	3.31E-03	6.50E-03
XVAE + FS	XVAE (corr 0.3)	0.203	0.225	0.217	0.727	0.117	1.98	0.212	0.307	7.05E-03	1.23E-02
	XVAE (corr 0.5)	0.203	0.225	0.217	0.761	0.0842	2.31	0.339	0.482	4.00E-03	7.38E-03
	XVAE (pVal 0.05)	-	-	-	-	-	-	-	-	-	-
cXVAE	input	0.197	0.217	0.209	0.66	0.106	2.33	0.0961	0.129	2.36E-01	4.14E-01
	inputEmbed	0.195	0.218	0.209	0.873	0.0877	2.43	0.443	0.53	1.47E-03	5.22E-03
	embed	0.195	0.216	0.208	0.9	0.109	2.43	0.657	0.742	8.35E-04	3.65E-03
	fusedEmbed	0.191	0.216	0.206	0.829	0.101	2.38	0.575	0.680	3.76E-04	2.96E-03
adv-XVAE	multiclass	0.204	0.225	0.217	0.707	0.123	2.15	0.254	0.298	1.29E-01	2.48E-01
	multiclass (1batch)	0.263	0.286	0.277	0.777	0.146	2.05	0.140	0.193	1.36E-01	3.37E-01
	multiclass (scGAN)	0.196	0.218	0.210	0.681	0.111	2.41	0.0115	0.0102	3.58E-01	5.92E-01
	multinet	-	-	-	-	-	-	-	-	-	-
cr-XVAE	corrSq	0.200	0.222	0.213	0.744	0.079	2.380	0.206	0.314	3.78E-02	9.69E-02
	corrAbs	0.201	0.223	0.214	0.704	0.093	2.410	0.205	0.279	1.31E-01	2.51E-01
	MIhist	0.204	0.223	0.215	0.755	0.090	2.310	0.393	0.532	2.09E-03	6.24E-03
	MIKDE	0.202	0.225	0.216	0.815	0.091	2.280	0.319	0.469	2.15E-03	5.81E-03

multiple confounders

						Clustering performance									
		reconstruction error			CC	Internal		True label		Linear conf.		Non-linear conf.		Categorical conf.	
		X1	X2	X1,X2	dispersion	Silhouette	DB index	ARI	NMI	ARI	NMI	ARI	NMI	ARI	NMI
XVAE	mean	0.145	0.174	0.161	0.725	0.077	2.441	0.216	0.269	1.50E-02	2.57E-02	1.40E-01	1.97E-01	6.72E-02	1.33E-01
	std	0.004	0.002	0.003	0.043	0.006	0.058	0.089	0.100	1.93E-02	3.03E-02	4.33E-02	4.71E-02	4.77E-02	8.20E-02
XVAE + FS	mean	0.145	0.174	0.161	0.731	0.089	2.341	0.265	0.327	7.17E-03	1.20E-02	1.91E-02	2.78E-02	1.09E-01	2.03E-01
	std	0.004	0.002	0.003	0.037	0.006	0.064	0.085	0.104	8.63E-03	1.06E-02	2.99E-02	3.97E-02	5.75E-02	9.60E-02
cXVAE	mean	0.130	0.159	0.146	0.905	0.126	2.243	0.634	0.713	1.25E-04	2.69E-03	-3.67E-04	2.18E-03	4.62E-04	3.35E-03
	std	0.003	0.002	0.002	0.022	0.009	0.065	0.042	0.031	3.83E-04	5.10E-04	4.68E-04	5.78E-04	5.01E-04	7.26E-04
adv-XVAE	mean	0.141	0.172	0.158	0.753	0.106	2.207	0.225	0.262	1.56E-02	2.58E-02	1.07E-01	1.51E-01	1.06E-01	2.22E-01
	std	0.003	0.005	0.004	0.066	0.008	0.054	0.120	0.130	2.28E-02	3.48E-02	5.23E-02	7.37E-02	5.14E-02	1.04E-01
cr-XVAE	mean	0.145	0.174	0.161	0.764	0.095	2.234	0.369	0.490	2.67E-03	6.91E-03	6.88E-03	1.71E-02	4.87E-04	3.47E-03
	std	0.005	0.002	0.003	0.031	0.007	0.074	0.064	0.064	1.74E-03	3.58E-03	1.05E-02	2.44E-02	5.02E-04	7.75E-04

Supplementary Table 3: **Overview performances of deconfounding strategy for multiple confounder simulations**

No. of iterations	CC dispersion	Internal clustering		True clustering		Confounder clustering	
		Silhouette	DB index	ARI	NMI	ARI	NMI
10	0.847	0.100	2.373	0.580	0.686	3.48E-04	2.95E-03
50	0.834	0.100	2.379	0.575	0.681	6.23E-04	3.22E-03
100	0.842	0.100	2.377	0.575	0.680	5.42E-04	3.15E-03
150	0.843	0.100	2.377	0.575	0.681	4.98E-04	3.12E-03
200	0.847	0.100	2.373	0.575	0.680	6.29E-04	3.27E-03
	0.843	**0.100**	**2.376**	**0.576**	**0.682**	**5.28E-04**	**3.14E-03**
	(± 5.32E-03)	(± 0)	(± 2.68E-03)	(± 2.24E-03)	(± 2.51E-03)	(± 1.15E-04)	(± 1.22E-04)

Supplementary Table 4: **Overview performances of cXVAE for different numbers of sampled embedding**. This experiment was done using the *fusedEmbed* version of cXVAE on the TCGA data with artificial categorical confounders. We tried with various numbers (10,50,100,150,200) of sampling the embedding from the latent distributions of cXVAE. Values below the doubled line are the mean (in bold) and standard deviation (within brackets) of each column.